Temporally Dependent Rate-Distortion Optimization for Low-Delay Hierarchical Video Coding

Yanbo Gao, Ce Zhu, *Fellow, IEEE*, Shuai Li, and Tianwu Yang

***Abstract*— Low-delay hierarchical coding structure (LD-HCS), as one of the most important components in the latest High Efficiency Video Coding (HEVC) standard, greatly improves coding performance. It groups consecutive P/B frames into different layers and encodes them with different quantization parameters (QPs) and reference mechanisms in such a way that temporal dependency among frames can be exploited. However, due to varying characteristics of video contents, temporal dependency among coding units differs significantly from each other in the same or different layers, while a fixed LD-HCS scheme cannot take full advantage of the dependency, leading to a substantial loss in coding performance. This paper addresses the temporally dependent rate distortion optimization (RDO) problem by attempting to exploit varying temporal dependency of different units. First, the temporal relationship of different frames under the LD-HCS is examined, and hierarchical temporal propagation chains are constructed to represent the temporal dependency among coding units in different frames. Then, a hierarchical temporally dependent RDO scheme is developed specifically for the LD-HCS based on a source distortion propagation model. Experimental results show that our proposed scheme can achieve 2.5% and 2.3% BD-rate gain in average compared with the HEVC codec under the same configuration of P and B frames, respectively, with a negligible increase in encoding time. Furthermore, coupled with QP adaption, our proposed method can achieve higher coding gains, e.g., with multi-QP optimization, about 5.4% and 5.0% BD-rate saving in average over the HEVC codec under the same setting of P and B frames, respectively.**

***Index Terms*— Low-delay hierarchical coding structure, HEVC, temporal dependency, rate-distortion optimization.**

I. Introduction

THE latest High Efficiency Video Coding (HEVC) [1] standard significantly improves coding efficiency compared to the precedent standards. For example, compared to H.264/AVC [2], it provides a rate reduction of approximately 50% while achieving equal video quality. Many techniques, including tree-structured block partition [3], merge mode [4], more intra modes [5], sample adaptive offset (SAO) filter [6] and hierarchical coding structure (HCS) [7]–[9], have been adopted, which leads to its superior performance. Among them, HCS groups P/B frames into different temporal layers and frames in the same layer are coded with the same and fixed strategy in selecting the quantization parameter (QP) and the reference frames while frames in different layers are coded with different strategies. Fig. 1 shows an example of HCS under the Low-Delay (LD) configuration (noted as LD-HCS hereafter in this paper), where frames are encoded interlacedly with relatively large and small QP values, resulting in low and high reconstruction quality, respectively. As we know, due to the widely used inter prediction mechanism in the modern coding standards, coding of one P/B frame is highly dependent on its reference frames. To exploit this temporal dependency, frames with high reconstruction quality in the lowest temporal layer (layer 1 in Fig. 1) are included into the reference frame set more frequently than other frames to improve the motion compensation efficiency. However, video contents are generally different from each other and even in one video sequence, different portions of the video frames generally show different characteristics which results in varying optimal coding behaviors for different portions. Thus, a predefined coding structure using a fixed QP selection and a fixed reference management scheme as in the current HEVC codec cannot achieve optimal coding globally.

A number of approaches working on the coding structure have been reported in literature. In [10], a long-term reference frame with high quality is inserted adaptively based on the RD performance analysis of motion compensated prediction based on the coded frames without considering the temporal relationship of the whole sequence. Li *et al.* [8] reformulated the reference picture management as an optimization problem and attempted to obtain an optimal solution by Viterbi algorithm by traversing all possible solutions. In [11], a new QP refinement (QPR) scheme is developed based on the relationship between Lagrange multiplier and QP under HCS. Furthermore, with a fixed Lagrange multiplier, multi-QP (MQP) optimization [12] is integrated in the HEVC where QP values in a predefined set are tested in the mode decision process and the one with the smallest RD cost is selected for the final coding. The encoding time is almost equivalent to that of encoding a sequence multiple times using different QPs, which greatly aggravate the computation burden. In [13], QP cascading (QPC) in HCS was formulated as a non-

Manuscript received September 17, 2016; revised March 13, 2017 and April 17, 2017; accepted May 5, 2017. Date of publication June 8, 2017; date of current version July 6, 2017. This work was supported in part by the National Natural Science Foundation of China under Grant 61571102 and in part by the Other Funds under Grant 2015AA015903 and Grant ZYGX2014Z003. The associate editor coordinating the review of this manuscript and approving it for publication was Dr. Yui-Lam Chan. *(Corresponding author: Ce Zhu.)*

Y. Gao and C. Zhu are with the School of Electronic Engineering, University of Electronic Science and Technology of China, Chengdu 611731, China, and also with the Center for Robotics, University of Electronic Science and Technology of China, Chengdu 611731, China (e-mail: yanbogao@std.uestc.edu.cn; eczhu@uestc.edu.cn).

S. Li is with the University of Wollongong, Wollongong 2500, Australia (e-mail: shuailichn@gmail.com).

T. Yang is with the Advanced Robotics and Intelligent Control Centre, Singapore Polytechnic, Singapore 139651 (e-mail: yangtw@sp.edu.sg).

Color versions of one or more of the figures in this paper are available online at http://ieeexplore.ieee.org.

Digital Object Identifier 10.1109/TIP.2017.2713598

linear programming problem, and QP values are adaptively obtained for each frame considering temporal dependency. Although the above frame-level reference and QP selection methods may improve coding efficiency, they still treat units in a frame the same and perform rate-distortion optimization (RDO) [14], [15] without a comprehensive consideration of dependency among different units.

There are some works related to the spatially/temporally dependent RDO (SD-RDO or TD-RDO) which consider the effect of coding one unit on others due to prediction-induced dependency [16]. A general framework [17] was proposed to minimize the RD cost by jointly considering motion estimation, quantization and entropy coding. The core of this framework is the graph-based algorithm for near optimal soft decision quantization (SDQ) implemented by dynamic programming. In [18], a transform coefficient level selection method was proposed to iteratively update the motion estimation and quantization based on a linear signal model. In [19], the dependent RDO problem was solved using the primal-dual decomposition scheme and the subgradient projection method. The dependency was processed in the master primal problem and accordingly the RD cost of units can be minimized independently by the dual decomposition. The optimal Lagrange multiplier was iteratively updated by the solution of the corresponding dual problem. In [20] the authors proposed a PixelRank model based on PageRank to estimate the importance of each pixel on all the other pixels that refer to the pixel. Then an MB-based quantization parameters adjustment method was used to perform bit allocation based on the PixelRank scores. However, this method requires obtaining the PixelRank scores before the actual encoding, which leads to a two-pass encoding. It has been shown that these RDO approaches are very time-consuming due to the iterations or the dynamic programming, which makes them be infeasible in applications like real-time encoding. It is known that the coding efficiency of inter prediction is generally much higher than that of intra prediction and the resulting temporal dependency is consequently substantially stronger than the spatial dependency. Therefore, this paper only considers the temporal dependency while the relatively weaker spatial dependency is ignored.

It is worth noting that our previous conference paper [21] introduced a temporally dependent RDO method under the regular IPPP/IBBB coding structure in H.264/AVC, where a source distortion temporal propagation (SDTP) model was developed to consider the effect of the temporal dependency in the RDO process. In H.264/AVC, P/B frames are encoded using the same QP and the same reference selection scheme, making the temporal propagation relationship simple and largely tractable. Generally, each unit only directly affects one unit in the next frame and then propagates further from that unit. However, in the new standard of HEVC, HCS is introduced which greatly complicates the temporal propagation relationship, in view that P/B frames are grouped into different layers and encoded with different reference selection strategies coupled with varying QP assignment. The tracking of units affected by the to-be-coded unit becomes significantly complicated as multiple units in different frames may be directly affected by the to-be-coded unit which further disperses the propagation. In our previous work [22], [23], a Lagrange multiplier adaptation method considering inter-frame dependency was proposed under high-rate assumption. The method was developed using the high-rate distortion approximation, which circumvents the issue of distortion propagation, thus greatly simplifying the dependent RDO formulation by only modeling the inter-frame rate relationship. Moreover, to mitigate the deviation effect in the case of moderate or low coding rates, a regulation mechanism was employed to further rectify the Lagrange multiplier. In this paper, we consider a more general formulation to perform the temporally dependent rate distortion optimization, which instead aims to model distortion propagation in the temporal domain under the hierarchical coding structure.

To address the temporally dependent RDO for the hierarchical coding structure in HEVC, especially for the LD-HCS in HEVC, a hierarchical temporally dependent RDO method is presented in this paper, which considers the hierarchical temporal dependency among units. First, the temporal relationship among frames is examined under the LD-HCS and a hierarchical temporal propagation chain is constructed by identifying the temporally correlated units. Based on the constructed hierarchical temporal propagation chain, the TD-RDO is reformulated as the optimization of cross-layer distortions of temporally related units and the associated rate. A source distortion temporal propagation model for units in each layer is developed to solve the TD-RDO. It is shown that the proposed TD-RDO can be implemented by updating Lagrange multipliers for different units in different layers. Experimental results show that the proposed method can achieve BD-rate reductions of 2.5% and 2.3% in average under the LD configuration of P and B frames, respectively. Moreover, better performance can be obtained by refining QP according to the updated Lagrange multipliers. Specifically, compared with the reference software of HEVC codec, our proposed method achieves BD-rate savings of 3.6% and 3.2% in average coupled with QP refinement [11], and BD-rate saving of 5.4% and 5.0% together with MQP [12] under the LD configuration of P and B frames, respectively.

Part of this work has been published in our previous 4-page conference paper [24], which only presents the basic idea of dealing with temporally dependent RDO under the LD-HCS. In this paper, a comprehensive analysis of our proposed temporally dependent RDO method is made and a couple of new techniques are further presented to improve coding performance including the adaptive updating of reference utilization rate. More experimental results and justifications with insightful discussions are provided to shed light on our proposed method.

The rest of the paper is organized as follows. In Section II, hierarchical temporally dependent RDO is formulated for the LD-HCS based on a hierarchical temporal propagation chain. Section III presents the hierarchical source distortion temporal propagation model for units in different layers. Experimental results are presented in Section IV, and finally, conclusions are drawn in Section V.

II. Hierarchical Temporally Dependent RDO Formulation Under Low-Delay Video Coding

As in our previous work [21], temporally dependent RDO can be represented as

$$\min_{o_1,\ldots,o_N}\left(\sum_{i=1}^{N} D_i(o_1,o_2,\ldots,o_i)+\lambda_g\cdot\sum_{i=1}^{N} R_i(o_1,o_2,\ldots,o_i)\right) \tag{1}$$

where λ_g is the global Lagrange multiplier, and o_i is the coding option of the *i-th* coding unit, including coding mode, motion vector, reference frame index, quantization parameter and quantized transform coefficients. R_i and D_i denote the rate and distortion of the coding unit i, respectively. N coding units are assumed to be temporally related units located in N frames respectively.

When considering the optimization of coding a unit U_i, the temporally dependent RDO can be simplified as

$$\min_{o_i}\left(\sum_{j=i}^{N} D_j(o_i,o_{i+1}^*,\ldots,o_j^*)+\lambda_g R_i(o_i)\right) \tag{2}$$

where $(o_{i+1}^*,\ldots,o_j^*)$ are denoted as optimal coding options for units $U_{i+1},\ldots,U_j$, respectively. The simplification is made based on two considerations: 1) When considering the optimization of U_i, coding of the units in the frames before U_i is already completed and accordingly the corresponding coding options $(o_1,o_2,\ldots,o_{i-1})$ are deterministic and not related to the current coding unit U_i, which are then all removed; 2) Ignoring the spatial dependency, the rate of the current unit is only determined by its own coding option, which contains all the information to be coded in the entropy coding stage, that is $R_i(o_1,o_2,\ldots,o_i)=R_i(o_i)$, thus decoupling the rate dependency. More justifications on the simplification can be found in our previous work [21]. Based on the above formulation, only the rate of the current unit and the distortions of the current unit and the subsequent units temporally related to and affected by U_i are to be evaluated.

A. Hierarchical Temporal Propagation Chain Under LD-HCS

To address the above TD-RDO problem under LD-HCS, the temporal relationship introduced by inter-prediction is examined first to identify all the temporally related units. In the default LD-HCS in the HEVC, all the P/B frames in a sequence are partitioned into sequential groups of pictures (GOP). Each GOP contains a fixed number of frames (four by default), which are further divided into three different temporal layers as shown in Fig. 1. The number associated with each frame represents the display order noted as POC (picture order count) which equals its encoding order in the LD-HCS. Frames in one GOP can be identified by the relative POC (rPOC) from 1 to 4 in Fig. 1, and frames with the same rPOC in different GOPs share the same scheme on the QP value selection and reference management as tabulated in TABLE I. Delta QP values are used to obtain the QP values (by adding QP of I frame) in coding the P/B frames of different layers. As shown in Fig. 1, QP value increases with the temporal layer. Specifically, among all the P/B frames, the smallest QP value is assigned to the frames in the lowest temporal layer (noted as key frames), i.e., temporal layer 1, leading to the highest reconstruction quality among all the P/B frames. TABLE I also tabulates the reference frame set in the LD-HCS where Delta POC represents the difference between the POC of reference frame and that of the current frame. It can be seen that the reference frame set contains four frames including the immediately previous frame, which is the closest to the current frame, and the three previous key frames, which may provide a high quality motion-compensated prediction.

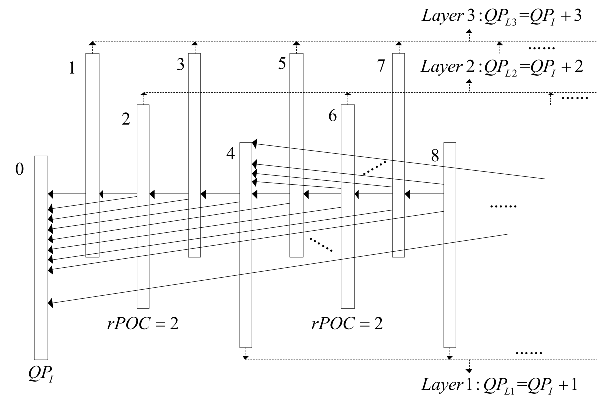

Fig. 1. Hierarchical coding structure under Low-Delay configuration.

TABLE I
DELTA QPs AND REFERENCE FRAME SETS UNDER LD-HCS IN THE HEVC

rPOC	Delta POC				Delta QP
	Ref 1	*Ref 2*	*Ref 3*	*Ref 4*	
1	-1	-5	-9	-13	3
2	-1	-2	-6	-10	2
3	-1	-3	-7	-11	3
4	-1	-4	-8	-12	1

TABLE II
AVERAGE UTILIZATION RATES OF THE FOUR P FRAMES IN THE REFERENCE FRAME SET UNDER LD-HCS, RESPECTIVELY

rPOC	Reference Utilization Rate (in Percentage)			
	Ref 1	*Ref 2*	*Ref 3*	*Ref 4*
1	0.89	0.05	0.02	0.01
2	0.70	0.20	0.04	0.02
3	0.79	0.12	0.04	0.02
4	0.62	0.19	0.06	0.04

With extensive simulations, the average utilization percentages of reference frames with respect to each frame in a GOP (noted as reference utilization rates) are shown in TABLE II for P frames in the LD-HCS (similar observations can be found for B frames). As in TABLE II, units in each P frame are mostly predicted from and thus heavily affected by the immediately previous frame (*Ref 1*) and the nearest key frame (*Ref 2*) if *Ref 1* is not a key frame. By ignoring the weaker prediction relationships from the other reference frames corresponding to small utilization rates, the hierarchical temporal propagation relationship can be presented as in Fig. 2,

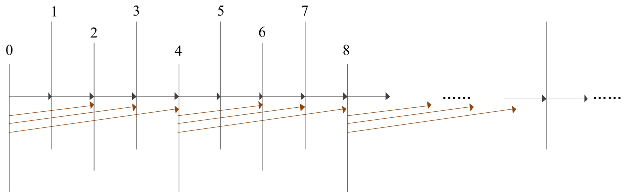

Fig. 2. Illustration of a simplified hierarchical temporal propagation relationship under the LD-HCS.

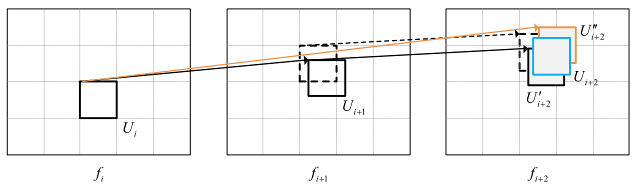

Fig. 3. Construction of the hierarchical temporal propagation chain under the LD-HCS.

where the arrows indicate effective prediction/propagation relationship.

Based on the above hierarchical temporal propagation relationship, the temporally related units can be identified using forward motion search on the original frames as in our previous work [21] in order to construct a hierarchical temporal propagation chain. In H.264/AVC, each unit only directly affects one unit in the next frame and indirectly influences the others subsequently encoded. Thus the units not in the immediately following frame can only be indirectly affected by the current unit through those between them. However, under the LD-HCS, the units may still be directly affected by the current unit as described in the hierarchical temporal propagation relationship. Accordingly the identification of temporally related units becomes more complex compared with that in [21].

Taking a unit in the key frame f_i, denoted by U_i with a solid square shown in Fig. 3 as an example. According to the hierarchical temporal propagation relationship in Fig. 2, f_i may affect the coding performance of frame f_{i+2} by indirectly affecting U'_{i+2} (through U_{i+1}) or directly affecting unit U''_{i+2}. When continuing to identify the affected units in the following frames by U'_{i+2} and U''_{i+2}, the temporal propagation is further dispersed with more branches, thus becoming more complicated. In view that U'_{i+2} and U''_{i+2} are both predicted from U_i directly or indirectly, they are supposed to be very close to each other if not being identical. To avoid such complicated tracking of temporally affected units in the following frames, a unit U_{i+2} which covers most of U'_{i+2} and U''_{i+2} is taken as the affected unit, marked with a blue square in Fig. 3. Then that unit U_{i+2} is treated as the "merged" node in the chain to be used to identify the temporally affected units in the subsequent frames, thus greatly simplifying the construction of temporal propagation chain.

The above process may still be very time-consuming if motion search is performed each time to construct the temporal propagation chain when coding one unit. To further save computational complexity in the chain construction, frames are first divided into non-overlapped "coding" units and motion search is only performed for such "coding" units as in Fig. 3. For a unit identified to be affected that rides across several "coding" units, its motion information is approximated to be the motion of the "coding" unit (marked with dotted border in Fig. 3) that covers the most area of the affected unit. In this way, motion search complexity can be reduced significantly.

B. Hierarchical Temporally Dependent RDO Formulation

As mentioned in Section II.A, a unit may be predicted from different reference frames resulting in different coding distortions. Accordingly the distortion of each related unit in (2) is estimated as the expectation in view of the different prediction results. The hierarchical TD-RDO can thus be described as

$$\min_{o_i}\left(\sum_{j=i}^{N} E(D_j(o_i, o^*_{i+1}, \ldots, o^*_j)) + \lambda_g R_i(o_i)\right) \tag{3}$$

where $E(D_j(o_i, o^*_{i+1}, \ldots, o^*_j))$ is the expected distortion of coding unit U_j under different predictions. It can be seen that to tackle the above RDO problem with respect to o_i, only the distortions affected by o_i need to be estimated, which are detailed as follows.

1) Problem Formulation for Units in Key Frames: First we consider the coding of unit U_i in a key frame f_i. Note that for the current unit, the expected distortion $E(D_i(o_i))$ is $D_i(o_i)$ since the coding of its reference frames is completed and the influence propagated to U_i is deterministic based on the testing option o_i. As in (3), to perform the TD-RDO for the current unit, the distortions of the following related units (starting from the affected unit U_{i+1} in the next frame f_{i+1} with rPOC = 1) need to be estimated. Considering all the possible predictions according to the reference mechanism specified in TABLE I with the GOP size of 4 (which is the case considered throughout the paper unless otherwise specified), the expected distortion $E(D_{i+1}(o_i, o^*_{i+1}))$, denoted as $E(D_{i+1})$ for short, can be obtained as

$$\begin{aligned} E(D_{i+1}) = {} & P_{i,i+1} \cdot D_{i+1}(o_i, o^1_{i+1}) + P_{i-4,i+1} \\ & \cdot D_{i+1}(o_{i-4}, o^2_{i+1}) + P_{i-8,i+1} \cdot D_{i+1}(o_{i-8}, o^3_{i+1}) \\ & + P_{i-12,i+1} \cdot D_{i+1}(o_{i-12}, o^4_{i+1}) \end{aligned} \tag{4}$$

where o^h_{i+1} represents the coding option of U_{i+1} if $Refh$, with the frame index $idx(Refh) = i, i-4, i-8, i-12$, is selected as the reference. $P_{idx(Refh),i+1}$ is the probability of unit U_{i+1} using $Refh$ as the reference frame, which is estimated as the utilization rate of $Refh$ referenced by f_{i+1}. For example, o^1_{i+1} represents the coding option when $Ref1$, i.e. f_i, in the reference frame set is selected as the reference frame. $P_{i,i+1}$ can be obtained as the utilization rate of f_i referenced by f_{i+1}. $D_{i+1}(o_i, o^1_{i+1})$ represents the distortion of the affected unit U_{i+1} when referring to U_i (its coding option is o_i) in the reference frame f_i. $D_{i+1}(o_{i-4}, o^2_{i+1})$ is the distortion of the affected unit U_{i+1} when referring to U_{i-4} (its coding option is o_{i-4}) in the reference frame f_{i-4}, which is $Ref2$ in its reference frame set.

When optimizing the coding of unit U_i, we only need to consider the terms that are related to o_i. Then $D_{i+1}(o_i, o^1_{i+1})$

needs to be obtained and (4) becomes

$$E(D_{i+1}) = P_{i,i+1} \cdot D_{i+1}(o_i, o_{i+1}^1) + K_{i+1} \quad (5)$$

where K_{i+1} represents the last three terms in (4), which are independent of o_i.

Likewise, for the affected unit U_{i+2} in the frame f_{i+2} with rPOC = 2, the expected distortion can be obtained as

$$E(D_{i+2}) = P_{i+1,i+2} \cdot D_{i+2}(o_i, o_{i+1}^*, o_{i+2}^1) + P_{i,i+2} \cdot D_{i+2}(o_i, o_{i+2}^2) + K_{i+2} \quad (6)$$

where $K_{i+2} = P_{i-4,i+2} \cdot D_{i+2}(o_{i-4}, o_{i+2}^3) + P_{i-8,i+2} \cdot D_{i+2}(o_{i-8}, o_{i+2}^4)$ is independent of o_i. $D_{i+2}(o_i, o_{i+1}^*, o_{i+2}^1)$ and $D_{i+2}(o_i, o_{i+2}^2)$ are the distortions of the affected unit U_{i+2} when using its immediately previous frame f_{i+1} and its nearest key frame f_i as the reference, respectively. Distortions of the affected units U_{i+3} and U_{i+4} can be obtained in a similar way which is shown in Appendix A.

For the units in the following GOPs, frame f_i is no longer their nearest key frame reference, and accordingly they will not be directly affected from the distortion $D_i(o_i)$ as indicated by the hierarchical temporal propagation relationship. The effect of encoding the unit U_i, i.e., distortion $D_i(o_i)$, will be propagated to the units in the next GOP through its effect on its following units in the current GOP, and then further propagated to the following GOPs.

Here we consider the expected distortion of the affected unit U_{i+4m+1} in the *m-th* GOP. Note that m indicates the index of a GOP where the affected unit U_{i+4m+1} is located and assumably there are totally M affected GOPs in the sequence when coding U_i. Based on the above discussion, for U_{i+4m+1}, only the effect of its immediately previous frame is considered and thus $E(D_{i+4m+1})$ can be expressed as $P_{i+4m,i+4m+1} \cdot D_{i+4m+1}(o_i, o_{i+1}^*, \ldots, o_{i+4m}^*, o_{i+4m+1}^1) + K_{i+4m+1}$, where $D_j(o_i, o_p^*, \ldots, o_q^*, o_j^1)$ denotes the coding distortion of unit U_j indirectly affected by coding option o_i through the coding units $U_p, \ldots, U_q$ with the coding option $o_p^*, \ldots, o_q^*$, respectively. K_{i+4m+1} represents the three terms corresponding to the other three reference frames, f_{i+4m-4}, f_{i+4m-8}, $f_{i+4m-12}$. As shown in TABLE II, the utilization rates of the other three reference frames are very small for rPOC = 1, resulting in trivial influence. For simplification, these terms are not taken into account in the estimation of influence of o_i on the distortion of U_{i+4m+1}. Other expected distortions, i.e., $E(D_{i+4m+2})$, $E(D_{i+4m+3})$, $E(D_{i+4m+4})$, in the GOP can be similarly obtained based on the above discussion. For example, $E(D_{i+4m+2})$ can be represented as

$$\begin{pmatrix} P_{i+4m+1,i+4m+2} \cdot D_{i+4m+2}(o_i, o_{i+1}^*, \ldots, o_{i+4m+1}^*, \\ o_{i+4m+2}^1) + P_{i+4m,i+4m+2} \cdot D_{i+4m+2}(o_i, o_{i+1}^*, \ldots, o_{i+4m}^*, \\ o_{i+4m+2}^2) + K_{i+4m+2} \end{pmatrix},$$

where K_{i+4m+2} are assumed unrelated to o_i since their corresponding reference utilization rates are very small and their influence can be ignored.

2) Problem Formulation for Units in Non-Key Frames: The above presents the influence of coding the current unit U_i on the following affected units in terms of distortion propagation, assuming U_i is located in a key frame.

Now we consider coding the unit in the first non-key frame (rPOC = 1) in a GOP, as an example. To be consistent with the above analysis for the unit U_i in the key frame f_i, we denote the non-key frame with rPOC = 1 by f_{i+1} and the unit in the frame by U_{i+1}. To optimize the coding of unit U_{i+1}, the hierarchical TD-RDO problem in (3) becomes

$$\min_{o_{i+1}} \left(\sum_{j=i+1}^{N} E(D_j(o_{i+1}, o_{i+2}^*, \ldots, o_j^*)) + \lambda_g R_{i+1}(o_{i+1}) \right) \quad (7)$$

where all the expected distortions of the affected units are evaluated by relating to the coding of the unit U_{i+1}.

We consider the following units (U_{i+2}, U_{i+3}, U_{i+4}) in the current GOP. For U_{i+2}, the expected distortion $E(D_{i+2})$ can be obtained as in (6)

$$E(D_{i+2}) = P_{i+1,i+2} \cdot D_{i+2}(o_{i+1}, o_{i+2}^1) + P_{i,i+2} \cdot D_{i+2}(o_i, o_{i+2}^2) + P_{i-4,i+2} \cdot D_{i+2}(o_{i-4}, o_{i+2}^3) + P_{i-8,i+2} \cdot D_{i+2}(o_{i-8}, o_{i+2}^4) \quad (8)$$

where the last three terms are unrelated to o_{i+1} and thus only the first term needs to be estimated. In the same way, we can obtain $E(D_{i+3})$, $E(D_{i+4})$ and the expected distortions of the affected units in the following GOPs, which will not be detailed here.

III. Hierarchical Source Distortion Propagation Model Under LD-HCS

Given the hierarchical TD-RDO formulation in the above section, the distortions of the units under different predictions need to be estimated, which is to be investigated in the following.

A. Source Distortion Propagation Model for Key Frames

First, we consider the optimization of the coding unit U_i in the key frame f_i. For the expected distortion $E(D_{i+1})$ shown in (5) of the affected unit U_{i+1} in the next frame f_{i+1}, only the first term $D_{i+1}(o_i, o_{i+1}^1)$ related to o_i needs to be estimated. Based on our previous work [21] and [25], distortion $D_{i+1}(o_i, o_{i+1}^1)$ of the affected unit U_{i+1} referring to f_i can be represented as

$$D_{i+1}(o_i, o_{i+1}^1) = e^{-b \cdot R_{i+1}(o_i, o_{i+1}^1)} \cdot D_{i+1}^{MCP}(o_i, o_{i+1}^1) = \alpha \cdot e^{-b \cdot R_{i+1}(o_i, o_{i+1}^1)} \cdot (D_i(o_i) + D_{i \to i+1}^{OMCP}) \quad (9)$$

where b is a constant related to the source distribution, and $R_{i+1}(o_i, o_{i+1}^1)$ is the coding rate of unit U_{i+1} only related to its own coding option o_{i+1}^1 as aforementioned, which may be rewritten as $R_{i+1}(o_{i+1}^1)$. $D_{i+1}^{MCP}(o_i, o_{i+1}^1)$ is the motion compensation predicted (MCP) error of coding unit U_{i+1} referring to U_i in f_i as reference frame, and can be approximated as $D_{i+1}^{MCP}(o_i, o_{i+1}^1) = \alpha \cdot (D_i(o_i) + D_{i \to i+1}^{OMCP})$, where α is experimentally set to be 0.94, and $D_{i \to i+1}^{OMCP}$ is the original

MCP (OMCP) error between U_i and U_{i+1} using forward motion search on the original frames (f_i and f_{i+1}), which is unrelated to o_i. Thus (5) can be expressed as

$$E(D_{i+1}) = P_{i,i+1} \cdot \beta_{i,i+1} \cdot D_i(o_i) + C_{i+1} \tag{10}$$

where

$$\beta_{i,i+1} = \alpha \cdot e^{-b \cdot R_{i+1}(o^1_{i+1})} \tag{11}$$

is considered to be independent of o_i, describing the factor of distortion propagation from a unit to its directly affected unit through MCP error. The term $C_{i+1} = \beta_{i,i+1} \cdot D^{OMCP}_{i \to i+1} + K_{i+1}$ can thus be removed as $\beta_{i,i+1} \cdot D^{OMCP}_{i \to i+1}$ and K_{i+1} are both unrelated to o_i.

For $E(D_{i+2})$, in (6), two terms need to be estimated. First, $D_{i+2}(o_i, o^*_{i+1}, o^1_{i+2})$ is the distortion of the affected unit U'_{i+2} in Fig. 3 when using U_{i+1} as reference. Together with (10), we can obtain

$$\begin{aligned} &D_{i+2}(o_i, o^*_{i+1}, o^1_{i+2}) \\ &\quad = \beta_{i+1,i+2} \cdot (E(D_{i+1}) + D^{OMCP}_{i+1 \to i+2}) \\ &\quad = \beta_{i+1,i+2} \cdot P_{i,i+1} \cdot \beta_{i,i+1} \cdot D_i(o_i) + C'_{i+2} \end{aligned} \tag{12}$$

$\beta_{i+1,i+2} = \alpha \cdot e^{-b \cdot R_{i+2}(o^1_{i+2})}$ and $C'_{i+2} = \beta_{i+1,i+2} \cdot (C_{i+1} + D^{OMCP}_{i+1 \to i+2})$ are the terms unrelated to o_i. $D^{OMCP}_{i+1 \to i+2}$ is the OMCP error between U_{i+1} and U'_{i+2}.

Likewise, the distortion $D_{i+2}(o_i, o^2_{i+2})$ of the affected unit U''_{i+2} when using U_i as reference can be expressed as

$$\begin{aligned} D_{i+2}(o_i, o^2_{i+2}) &= \beta_{i,i+2} \cdot (D_i(o_i) + D^{OMCP}_{i \to i+2}) \\ &= \beta_{i,i+2} \cdot D_i(o_i) + C''_{i+2} \end{aligned} \tag{13}$$

where $\beta_{i,i+2} = \alpha \cdot e^{-b \cdot R_{i+2}(o^2_{i+2})}$ and $C''_{i+2} = \beta_{i,i+2} \cdot D^{OMCP}_{i \to i+2}$ are unrelated to o_i. $D^{OMCP}_{i \to i+2}$ is the OMCP error between U_i and U''_{i+2}. Combining (12) with (13), the expected distortion of unit U_{i+2} can be obtained as

$$\begin{aligned} E(D_{i+2}) = &\ P_{i+1,i+2}\beta_{i+1,i+2} \cdot P_{i,i+1}\beta_{i,i+1} \cdot D_i(o_i) \\ &+ P_{i,i+2}\beta_{i,i+2} \cdot D_i(o_i) + C_{i+2} \end{aligned} \tag{14}$$

where $C_{i+2} = P_{i+1,i+2} \cdot C'_{i+2} + P_{i,i+2} \cdot C''_{i+2} + K_{i+2}$ is unrelated to o_i.

Similarly, the expected distortions of the following affected units in the GOP can be obtained, which is shown in Appendix A. Based on (10), (14), (A5) and (A8), all the expected distortions in the current GOP can be represented together as in (15), as shown at the bottom of this page, where $L_0 = \sum_{j=1}^{4} C_{i+j}$ is unrelated to o_i.

The expected distortions of the affected units in the next affected GOP can be obtained by treating U_{i+4} as the coding unit U_i. Accordingly, the aggregated expected distortions of the four affected units in the next affected GOP can be obtained as in (16), as shown at the bottom of this page, based on $E(D_{i+4})$, where $\sum_{j=1}^{4} \tilde{C}_{i+4+j}$ and L_1 represents all the terms unrelated to o_i.

More generally, we can obtain all the expected distortions of the affected units in the *m-th* subsequent GOP as in (17), as shown at the bottom of this page, also based on the expected distortion $E(D_{i+4m})$ (see (A10) in Appendix A), where L_m includes as all the terms unrelated to o_i.

$$\sum_{k=0}^{3} E(D_{i+k+1}) = \sum_{k=0}^{3} \left(\sum_{t=0}^{k} P_{i,i+k+1-t}\beta_{i,i+k+1-t} \cdot \prod_{j=i+k+1-t}^{i+k} P_{j,j+1}\beta_{j,j+1} \right) \cdot D_i(o_i) + L_0 \tag{15}$$

$$\begin{aligned} \sum_{k=0}^{3} E(D_{i+4+k+1}) &= \sum_{k=0}^{3} \left(\sum_{t=0}^{k} P_{i+4,i+4+k+1-t}\beta_{i+4,i+4+k+1-t} \cdot \prod_{j=i+4+k+1-t}^{i+4+k} P_{j,j+1}\beta_{j,j+1} \right) \cdot E(D_{i+4}) + \sum_{j=1}^{4} \tilde{C}_{i+4+j} \\ &= \sum_{k=0}^{3} \left(\sum_{t=0}^{k} P_{i+4,i+4+k+1-t}\beta_{i+4,i+4+k+1-t} \cdot \prod_{j=i+4+k+1-t}^{i+4+k} P_{j,j+1}\beta_{j,j+1} \right) \\ &\quad \cdot \left(\sum_{t=0}^{3} P_{i,i+4-t}\beta_{i,i+4-t} \cdot \prod_{j=i+4-t}^{i+3} P_{j,j+1}\beta_{j,j+1} \right) \cdot D_i(o_i) + L_1 \end{aligned} \tag{16}$$

$$\sum_{k=0}^{3} E(D_{i+4m+k+1}) = \left\{ \begin{aligned} &\sum_{k=0}^{3} \left(\sum_{t=0}^{k} P_{i+4m,i+4m+k+1-t}\beta_{i+4m,i+4m+k+1-t} \cdot \prod_{j=i+4m+k+1-t}^{i+4m+k} P_{j,j+1}\beta_{j,j+1} \right) \\ &\cdot \prod_{s=0}^{m-1} \left(\sum_{t=0}^{3} P_{i+4s,i+4s+4-t}\beta_{i+4s,i+4s+4-t} \cdot \prod_{j=i+4s+4-t}^{i+4s+3} P_{j,j+1}\beta_{j,j+1} \right) \end{aligned} \right\} \cdot D_i(o_i) + L_m \tag{17}$$

$$\begin{aligned} \sum_{j=1}^{N} E(D_j) = D_i(o_i) + \sum_{m=0}^{M} &\left\{ \begin{aligned} &\sum_{k=0}^{3} \left(\sum_{t=0}^{k} P_{i+4m,i+4m+k+1-t}\beta_{i+4m,i+4m+k+1-t} \cdot \prod_{j=i+4m+k+1-t}^{i+4m+k} P_{j,j+1}\beta_{j,j+1} \right) \\ &\cdot \prod_{s=0}^{m-1} \left(\sum_{t=0}^{3} P_{i+4s,i+4s+4-t}\beta_{i+4s,i+4s+4-t} \cdot \prod_{j=i+4s+4-t}^{i+4s+3} P_{j,j+1}\beta_{j,j+1} \right) \end{aligned} \right\} \\ &\cdot D_i(o_i) + L = (1 + \omega_i) \cdot D_i(o_i) + L \end{aligned} \tag{18}$$

Based on the above analysis of the distortion propagation, the expected distortions of all the affected units can be expressed as in (18), where L represents all the terms unrelated to o_i. ω_i is the aggregated propagation factor of current unit U_i, indicating the overall effecting factor of the current unit on all the following units affected directly or indirectly in terms of distortion propagation. Intuitively, the units with larger aggregated propagation factors need to be encoded with smaller distortions in order to reduce its effect on the following units.

By substituting (18), as shown at the bottom of the previous page, into (3), the hierarchical TD-RDO under the LD-HCS can be expressed (with a simple transform) as

$$\min_{o_i}\left(D_i+\lambda_g/(1+\omega_i)\cdot R_i\right) \tag{19}$$

where all the terms unrelated to o_i, such as L, are removed in that it is a minimization problem with regards to o_i. It can be seen that the hierarchical TD-RDO for a units in a key frame is boiled down to the form of conventional RDO with an adapted Lagrange multiplier, where the global Lagrange multiplier λ_g can be obtained according to our work in [21] and a brief introduction will be provided in Subsection III.C.

B. Source Distortion Propagation Model for Non-Key Frames

In a similar way, we can obtain the expected distortions of the following affected units when the current coding unit is located in a non-key frame. First we consider coding the unit U_{i+1} in the non-key frame f_{i+1} with rPOC = 1. For affected unit U_{i+2}, only the first term $D_{i+2}(o_{i+1},o^1_{i+2})$ in (8) needs to be estimated, which can be obtained as $\gamma_{i+1,i+2}\cdot\ (D_{i+1}(o_{i+1})+D^{OMCP}_{i+1\to i+2})$ according to (9) where $\gamma_{i+1,i+2}$ is not related to o_{i+1} and can be obtained in the same way as β. Then $E(D_{i+2})$ can be represented as

$$E(D_{i+2})=P_{i+1,i+2}\cdot\gamma_{i+1,i+2}\cdot D_{i+1}(o_{i+1})+I_{i+2} \tag{20}$$

where I_{i+2} represents all the terms unrelated to o_{i+1}.

In the same way, the expected distortion $E(D_{i+3})$ and $E(D_{i+4})$ for U_{i+3} and U_{i+4}, can be obtained in a similar form, respectively. All the three distortions can be expressed as

$$\begin{aligned}E(D_\upsilon)&=P_{i+1,i+2}\cdot\gamma_{i+1,i+2}\cdot\ldots\cdot P_{\upsilon-1,\upsilon}\cdot\gamma_{\upsilon-1,\upsilon}\cdot D_{i+1}(o_{i+1})+I_\upsilon\\&=\left(\prod_{j=i+1}^{\upsilon-1}P_{j,j+1}\gamma_{j,j+1}\right)\cdot D_{i+1}(o_{i+1})+I_\upsilon\end{aligned} \tag{21}$$

where $\upsilon=i+2,i+3,i+4$ and I_υ represents all the terms unrelated to o_{i+1}.

The sum of the three expected distortions in the current GOP becomes

$$\sum_{k=1}^{3}E(D_{i+k+1})=\sum_{t=i+1}^{i+3}\prod_{j=i+1}^{t}P_{j,j+1}\cdot\gamma_{j,j+1}\cdot D_{i+1}(o_{i+1})+J_0 \tag{22}$$

where J_0 represents all the terms unrelated to o_{i+1}. The effect of coding the unit U_{i+1} on the next GOP is propagated only through the unit U_{i+4} in the key frame considering that the other units in non-key frames are not used as reference for the units in the other GOPs. The propagation is similar to the distortion propagation of the units in the key frame, which is shown in (23), as shown at the bottom of this page, where $\sum_{j=1}^{4}\tilde{I}_{i+4+j}$ and J_1 represent all the terms unrelated to o_{i+1}. Likewise, the expected distortion of all the affected units in the following GOPs can be obtained.

By substituting expected distortions of all the affected units into (7), the TD-RDO for the units in the frame with rPOC = 1 can be expressed in a similar form of (19) with its aggregated propagation factor ω_{i+1} as in (24), as shown at the bottom of this page. The aggregated propagation factor for each coding

$$\begin{aligned}\sum_{k=0}^{3}E(D_{i+4+k+1})&=\sum_{k=0}^{3}\left(\sum_{t=0}^{k}P_{i+4,i+4+k+1-t}\gamma_{i+4,i+4+k+1-t}\cdot\prod_{j=i+4+k+1-t}^{i+4+k}P_{j,j+1}\gamma_{j,j+1}\right)\cdot E(D_{i+4})+\sum_{j=1}^{4}\tilde{I}_{i+4+j}\\&=\sum_{k=0}^{3}\left(\sum_{t=0}^{k}P_{i+4,i+4+k+1-t}\gamma_{i+4,i+4+k+1-t}\cdot\prod_{j=i+4+k+1-t}^{i+4+k}P_{j,j+1}\gamma_{j,j+1}\right)\\&\quad\cdot\left(\prod_{j=i+1}^{i+3}P_{j,j+1}\gamma_{j,j+1}\right)\cdot D_{i+1}(o_{i+1})+J_1\end{aligned} \tag{23}$$

$$\begin{aligned}\omega_{i+1}&=\sum_{t=i+1}^{i+3}\prod_{j=i+1}^{t}P_{j,j+1}\cdot\gamma_{j,j+1}\\&\quad+\sum_{m=1}^{M}\left[\begin{array}{l}\sum_{k=0}^{3}\left(\sum_{t=0}^{k}P_{i+4m,i+4m+k+1-t}\gamma_{i+4m,i+4m+k+1-t}\cdot\prod_{j=i+4m+k+1-t}^{i+4m+k}P_{j,j+1}\gamma_{j,j+1}\right)\\\cdot\prod_{s=1}^{m-1}\left(\sum_{t=0}^{3}P_{i+4s,i+4s+4-t}\gamma_{i+4s,i+4s+4-t}\cdot\prod_{j=i+4s+4-t}^{i+4s+3}P_{j,j+1}\gamma_{j,j+1}\right)\cdot\left(\prod_{j=i+1}^{i+3}P_{j,j+1}\gamma_{j,j+1}\right)\end{array}\right]\end{aligned} \tag{24}$$

unit in the other non-key frames can be obtained in the same way, which is not detailed here.

C. Estimation of Propagation Factors for Lagrange Multiplier Determination

Based on the above results, the hierarchical TD-RDO problem can be solved by adapting the global Lagrange multiplier in a unit level as in (19) with the aggregated propagation factor ω which indicates the effect of coding the unit on the following units. As in (18) and (24), ω is the aggregated propagation factor of the current unit to all its temporally related units, which can be obtained from β (for a key frame) and γ (for a non-key frame).

The estimation of β and γ is the same and hence we only take the estimation of β as an example. Combining (9) and (11), β can be represented as

$$\begin{aligned}\beta_{i,i+1} &= \alpha \cdot D_{i+1}(o_i, o^1_{i+1})/D^{MCP}_{i+1}(o_i, o^1_{i+1}) \\ &= D_{i+1}(o_i, o^1_{i+1})/(D_i(o_i) + D^{OMCP}_{i\to i+1}) \end{aligned} \quad (25)$$

According to our previous work [21], the relationship between the reconstruction distortion with a quantization step size Q and the corresponding MCP error can be expressed as

$$D = D^{MCP} \cdot F(\theta) \quad (26)$$

where $\theta = Q \cdot \sqrt{2/D^{MCP}}$ and $F(\theta) \in (0, 1]$, and $F(\theta)$ can be pre-estimated experimentally with varying Q using a larger number of coding units and be finally constructed as a look-up table with multiple entries of θ as in [21]

With the obtained table of $F(\theta)$, β can be obtained as

$$\beta = \alpha \cdot F(\theta) \quad (27)$$

once the MCP error (D^{MCP}) and the quantization step (Q) are known. As in (9), D^{MCP} of a coding unit is obtained based on the distortion of its referenced unit and the associated OMCP value between the unit and its referenced one. Based on (27) and (9), $\beta_{i,i+1} = \alpha \cdot F(\theta_{i,i+1})$ and $\theta_{i,i+1} = \sqrt{2}\, Q/\sqrt{\alpha \cdot (D_i(o_i) + D^{OMCP}_{i\to i+1})}$. Then $E(D_{i+1})$ can be obtained as in (10). Consequently, $\beta_{i+1,i+2}$ can be estimated since $E(D_{i+1})$ is available. Accordingly, all the following β value can be sequentially obtained by repeating the above processes and finally ω_i is known.

On the other hand, the global Lagrange multiplier needs to be estimated in order to perform the temporally dependent RDO. For the temporally dependent RDO, according to (19), the global Lagrange multiplier can be obtained as $\lambda_g = -(1+\omega_i) \cdot \partial D_i/\partial R_i$. In contrast, in the HEVC test model (HM), RDO is performed separately and independently for each unit, where $\lambda_{HM} = -\partial D^{HM}_i/\partial R^{HM}_i$. Note that under different RDO schemes, the distortions and rates are different. Based on the high rate distortion function in (9), λ_g and λ_{HM} can be expressed as $\lambda_g = (1+\omega_i) \cdot b \cdot D_i$ and $\lambda_{HM} = b \cdot D^{HM}_i$, respectively. Consequently, $\lambda_g \cdot D^{HM}_i = (1 + \omega_i) \cdot D_i \cdot \lambda_{HM}$. In the implementation of the proposed temporally dependent RDO, D^{HM}_i is not available, which is approximated by D_i obtained in the proposed RDO scheme. To mitigate the approximation effect as well as make the estimation more robust, λ_g may be determined with an averaged result based on all coded units available as follows

$$\lambda_g = \left(\sum_{i=1}^{n} (1 + \omega_i) \cdot D_i \Big/ \sum_{i=1}^{n} D_i\right) \cdot \lambda_{HM} \quad (28)$$

where n is the number of all the coded units available. To further facilitate our implementation, λ_g is updated every frame based on a sliding window, where the distortion sum is updated as the weighted sum of the aggregated distortion in the just encoded frame and the previously aggregated distortion with the weights of 1/8 and 7/8, respectively.

D. Implementation Details

From the implementation point of view, our algorithm can be summarized as follows. First, all the units affected by coding unit i (in a key frame) or $i + 1$ (in a non-key frame) are identified to construct the hierarchical temporal propagation chain as shown in Subsection II.A. Then the hierarchical temporally dependent RDO for unit i or $i + 1$ is formulated as minimizing the aggregated RD cost of unit i or $i + 1$ and the affected units as in (3) or (7). By using the developed hierarchical source distortion propagation model, all the expected distortions are obtained using the distortion of the current unit and β or γ such as in (10) or (20), where β or γ can be calculated as in Subsection III.C. Accordingly, the aggregated propagation factor ω is obtained as in (18) or (24) and the temporally dependent RDO problem for unit i or $i + 1$ can be solved independently in the form of (19). Some implementation details are listed in the following.

(1) Due to the multiple reference mechanism in the LD-HCS, the expected distortion $E(D)$ in (4) involves multiple distortions from different predictions. According to Section II.B, only distortions associated with high reference utilization rates are considered to obtain the expected distortion, where the utilization rates are to be normalized in calculating $E(D)$. Taking $E(D_{i+2})$ when encoding unit U_i in a key frame as an example, it can be approximated as $\tilde{E}(D_{i+2}) = \frac{P_{i+1,i+2}}{P_{i+1,i+2}+P_{i,i+2}} \cdot D_{i+2}(o_i, o^*_{i+1}, o^1_{i+2}) + \frac{P_{i,i+2}}{P_{i+1,i+2}+P_{i,i+2}} \cdot D_{i+2}(o_i, o^2_{i+2})$. Also the probabilities of selecting different reference frames are adaptively updated according to the coding statistics of the past frames, which shows slightly better performance than using constant utilization rates.

(2) Blocks of 16×16 are used as the basic unit in the forward motion search. Other sizes such as 32×32 also works for the algorithm but performs slightly worse according to our experimental results. An aggregated propagation factor is estimated for each basic unit first and then an overall aggregated propagation factor for a coding tree unit (CTU) of 64×64 is obtained as the average of all the 16×16 units located in the CTU. Also, the adapted Lagrange multiplier is clipped to the range of $(1/2{*}\lambda_{HM}, 2{*}\lambda_{HM})$ to avoid a dramatic change of bitrate among units.

Algorithm 1 summarizes the process of performing the proposed method for one CTU in a key frame. Similar process

TABLE III
CODING PERFORMANCE COMPARISON FOR THE LDP AND LDB CONFIGURATION IN TERMS OF LUMA BDBR (%)

Class	Sequence	QPC [13]		QPR [11]		HM+MQP [12]		Our previous work [24]		Prop		Prop+QPR		Prop+MQP	
		LDP	***LDB***	***LDP***	***LDB***	***LDP***	***LDB***	***LDP***	***LDB***	***LDP***	***LDB***	***LDP***	***LDB***	***LDP***	***LDB***
B	BasketballDrive	/	/	-1.5	-1.2	-2.2	-1.8	-2.3	-2.2	-2.3	-2.2	-4.1	-3.7	-5.5	-5.3
	BQTerrace	/	/	-1.3	-0.2	-1.9	-1.0	-1.2	-0.3	-1.4	-0.5	-1.6	0.0	-3.0	-1.7
	Cactus	/	/	-2.3	-1.7	-2.7	-2.0	-2.5	-2.3	-2.5	-2.3	-3.8	-3.2	-5.8	-5.1
	Kimono	/	/	-1.7	-1.2	-1.7	-1.3	0.2	0.7	-0.1	0.5	-1.8	-0.9	-2.6	-1.7
	ParkScene	/	/	-1.1	-0.9	-1.5	-1.2	-2.6	-2.7	-2.8	-2.9	-4.0	-4.0	-5.2	-5.3
	Average BDBR	/	/	**-1.6**	**-1.1**	**-2.0**	**-1.5**	**-1.7**	**-1.4**	**-1.8**	**-1.5**	**-3.0**	**-2.4**	**-4.4**	**-3.8**
C	BasketballDrill	-2.8	-2.9	-2.1	-1.6	-2.8	-2.5	-6.7	-6.3	-6.6	-6.0	-9.1	-8.4	-11.1	-10.4
	BQMall	-0.6	-0.7	-1.1	-0.8	-1.5	-1.3	-1.5	-1.8	-1.6	-1.8	-2.8	-2.8	-4.0	-4.1
	PartyScene	-2.4	-2.5	-1.5	-1.0	-1.9	-1.5	-1.7	-1.7	-1.7	-1.7	-2.9	-2.6	-4.0	-3.7
	RaceHorses	1.9	2.0	-1.5	-1.3	-2.0	-1.8	1.3	1.4	0.7	0.9	-0.3	0.0	-1.4	-1.2
	Average BDBR	**-1.0**	**-1.0**	**-1.5**	**-1.2**	**-2.0**	**-1.8**	**-2.2**	**-2.1**	**-2.3**	**-2.2**	**-3.8**	**-3.5**	**-5.1**	**-4.9**
D	BasketballPass	-0.2	-0.1	-1.9	-1.7	-2.3	-2.2	-2.0	-2.2	-2.0	-2.0	-4.6	-4.5	-5.8	-5.9
	BlowingBubbles	-1.9	-1.8	-1.2	-1.0	-1.5	-1.3	-1.6	-1.8	-1.7	-1.8	-2.9	-2.6	-3.7	-3.7
	BQSquare	-2.5	-2.0	-1.4	-0.5	-1.7	-1.3	0.6	0.9	0.2	0.6	-0.3	0.6	-1.2	-0.5
	RaceHorses	1.0	0.9	-1.3	-1.2	-1.8	-1.8	0.2	0.1	0.0	-0.1	-1.3	-1.3	-2.5	-2.4
	Average BDBR	**-0.9**	**-0.8**	**-1.4**	**-1.1**	**-1.8**	**-1.6**	**-0.7**	**-0.7**	**-0.9**	**-0.8**	**-2.3**	**-2.0**	**-3.3**	**-3.1**
E	FourPeople	/	/	-3.1	-2.7	-3.4	-3.0	-6.4	-6.4	-7.2	-6.9	-8.6	-7.7	-11.4	-10.7
	Johnny	/	/	-2.5	-1.7	-3.1	-2.1	-3.3	-2.8	-3.4	-2.7	-3.2	-2.4	-6.1	-4.9
	KristenAndSara	/	/	-3.4	-2.7	-3.4	-3.1	-4.6	-4.4	-4.8	-4.3	-4.4	-4.1	-8.6	-7.9
	Average BDBR	/	/	**-3.0**	**-2.3**	**-3.3**	**-2.7**	**-4.8**	**-4.5**	**-5.1**	**-4.7**	**-5.4**	**-4.7**	**-8.7**	**-7.8**
F	BaskeballDrillText	-3.0	-3.0	-2.0	-1.7	-2.7	-2.5	-5.7	-5.4	-5.4	-5.1	-7.2	-6.7	-9.5	-8.9
	ChinaSpeed	-2.4	-2.3	-2.1	-2.1	-2.8	-2.8	-2.3	-2.2	-2.1	-2.0	-2.9	-2.7	-5.2	-5.1
	SlideEditing	-0.3	-1.3	-0.5	-0.5	-2.6	-2.4	-0.1	-0.2	-0.2	-0.4	-0.2	-0.6	-3.2	-2.7
	SlideShow	-1.6	-1.6	-1.2	-0.9	-3.0	-2.8	-4.6	-4.7	-4.7	-4.5	-6.6	-6.4	-8.1	-8.0
	Average BDBR	**-1.8**	**-2.0**	**-1.5**	**-1.3**	**-2.8**	**-2.6**	**-3.2**	**-3.1**	**-3.1**	**-3.0**	**-4.2**	**-4.1**	**-6.5**	**-6.2**
Overall Average BDBR		**-1.2**	**-1.3**	**-1.7**	**-1.3**	**-2.3**	**-2.0**	**-2.4**	**-2.2**	**-2.5**	**-2.3**	**-3.6**	**-3.2**	**-5.4**	**-5.0**

Algorithm 1 Hierarchical Temporally Dependent RDO Procedure for One CTU in a Key Frame Under the LD-HCS

Objective: Estimate aggregated propagation factor ω_{ctu} of one CTU in a key frame and then perform temporally dependent RDO for the CTU

Initialization: Produce the basic units by dividing the CTU into non-overlapped units with size of 16x16

Repeating over each basic unit U_i :

1. Identify all the affected units ($U_{i+1}, U_{i+2}, U_{i+3}, \ldots, U_N$) in the temporal domain;
2. Based on (27), estimate $\beta_{i,i+1}$ and accordingly obtain the expected distortion $E(D_{i+1})$ of U_{i+1} as shown in (10);
3. Similarly, estimate $\beta_{i,i+2}$ and $\beta_{i+1,i+2}$ with $E(D_{i+1})$, and then obtain the expected distortion $E(D_{i+2})$ of U_{i+2} as shown in (14);
4. Sequentially estimate all the β values and the expected distortions $E(D)$ by repeating Step 2 and 3;
5. Obtain the aggregated propagation factor ω_i in (18) by substituting all the expected distortions into the temporal dependent RDO formulation in (3);

Performing the temporally dependent RDO for the CTU:

1. Average the aggregated propagation factors ω_i of the basic units in the CTU as the final aggregated propagation factor ω_{ctu} ;
2. Update the Lagrange multiplier used in HM with $\lambda_g/(1+\omega_{ctu})$, and λ_g is obtained as shown in (28).

can be applied for other CTUs in a non-key frame, which is not detailed here due to page limit.

IV. Experimental Results

We evaluate our proposed method against the state-of-the-art HEVC codec in terms of coding efficiency and complexity by incorporating our proposed method into the HEVC reference software HM 13.0.

A. Coding Performance Comparison

Common test conditions (CTC) [26] specified by JCT-VC are used as the simulation environment setting, and the Low-Delay P (LDP) and Low-Delay B (LDB) configurations are tested, respectively. 20 sequences of 8-bit depth are used in the test as suggested by the CTC, which includes four different resolution formats, i.e., 1080p (1920 × 1080), 720p (1280 × 720), SVGA (1024 × 768), WVGA (832 × 480), WQVGA (416 × 240) from Class B to Class F. In LD configuration, only the first frame is encoded as I frame. Four QP values (22, 27, 32, 37) are used for I frame and then a QP offset is introduced to obtain the final QP for each P/B frame. Specifically, the QP offset in LD configuration is (3, 2, 3, 1) for a cyclic GOP of four frames as default.

The rate-distortion performance of the proposed TD-RDO is measured in terms of BD-rate (BDBR) [27] over HM 13.0 as shown in TABLE III (column named "Prop"), where all the results under the LDP and LDB configuration are tabulated. It can be seen that the proposed method achieves BD-rate saving of 2.5% and 2.3% in average over HM 13.0 under the LDP and LDB configuration, respectively. It is worth noting that for sequences "FourPeople" and "BasketballDrill", over 6.0% BD-rate savings are achieved for both LDP and LDB configurations, which will be discussed with more details in

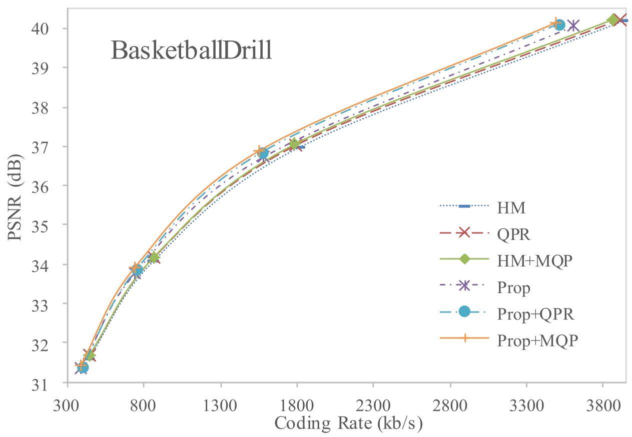

(a)

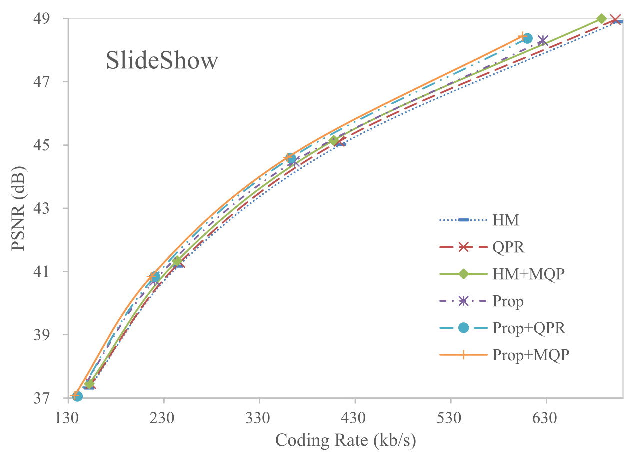

(b)

Fig. 4. RD curve comparison under the LDP configuration.

the following Subsection IV.B. Compared with our previous conference paper [24], some enhanced techniques developed in this paper, such as real-time updates of reference utilization, make the proposed method more robust with performance improvement of 0.1% BD-rate saving in average. From TABLE III, it can also be seen that our proposed method with the adapted Lagrange multiplier is superior to QP cascading scheme (QPC) [13] and QP refinement (QPR) [11], and even better than the high-complexity multiple QP (MQP) [12] (QP changes from -3 to 3).

It is known that the Lagrange multiplier is related to QP, and with an adapted Lagrange multiplier, better performance may be achieved by adapting QP accordingly. Therefore, further experiments were made using our proposed method with adapted QP values according to QPR and MQP, noted as “Prop+QPR” and “Prop+MQP” in TABLE III. It has shown that much better performance can be obtained compared to QPC, QPR and MQP methods which also adapt QP values. Particularly our proposed method together with MQP achieves over 5.4% and 5.0% BD-rate savings over the HEVC codec under the LDP and LDB configuration, respectively, which suggests the Lagrange multiplier obtained by our proposed method works the best with an appropriate QP found from MQP. Fig. 4 shows some examples of coding performance (RD curve) comparisons under the LDP configuration.

TABLE IV

Coding Performance (Luma BDBR) Under LDP and LDB Configurations for Sequences Captured Under Video Conference and Surveillance Settings

Type & Resolution		**Sequences Name**	**BDBR (%)**	
			LDP	***LDB***
Video Conference Setting	720P (1280x720)	Vidyo1	-3.6	-3.4
		Vidyo3	-1.4	-4.1
		Vidyo4	-4.5	-4.7
		Average BDBR	**-3.2**	**-4.1**
Surveillance Setting	SD (720x576)	Crossroad	-2.8	-3.1
		Office	-4.4	-5.0
		Overbridge	-6.1	-5.8
		Average BDBR	**-4.4**	**-4.6**
	HD (1600x1200)	Intersection	-7.6	-8.1
		Mainroad	-5.8	-7.2
		Average BDBR	**-6.7**	**-7.7**

The RD curves under LDB configuration are very similar to those of LDP and thus not presented again due to page limit.

B. More Comparisons and Discussions

It is known that the temporal dependency among units or frames in the sequences consisting of relatively stationary background with small motion, such as “FourPeople” and “BasketballDrill”, is stronger than other sequences with complex scenes and large motion like “RaceHorses”. Since our proposed method exploits temporal dependency to perform RDO, it naturally works better on the sequences with strong temporal dependency, which is clearly justified by the results on the relevant sequences like those in Class E in TABLE III). On the contrary, a small loss is observed for “RaceHorses” mainly due to the complex scenes and the large motion in the sequence leading to a poor exploitation of the temporal dependency.

To further validate that our proposed method works better on the sequences with strong temporal dependency, more experiments are conducted on some more stationary low-motion sequences as shown in TABLE IV. The sequences generally fall into two types captured under video conference and surveillance settings, respectively. The simulation setups such as QP and reference mechanism are the same as those in CTC. The coding results of the eight video sequences are tabulated in TABLE IV. For sequences under the video conference setting, the proposed method achieves an average of 3.2% and 4.1% BD-rate savings, under the LDP and LDB configuration, respectively. For sequences under the surveillance setting, the proposed method shows the average BD-rate gains of 4.4% and 4.6% for SD sequences, 6.7% and 7.7% for HD sequences, under the LDP and LDB configurations, respectively. Furthermore, for sequence “Intersection”, it achieves over 8% BD-rate saving under LDB configuration.

To gain more insights into our proposed method, the distribution of the adapted Lagrange multipliers is presented. Here we take the key frame with POC = 248 in “BassketballDrill” as an example, where six players run in circles and jump in turn to catch the rebound captured by a fixed camera. First, the distribution of the Lagrange multipliers in terms of differences between the adapted Lagrange multipliers and the original ones in HM13.0 for each CTU is shown in Fig. 5 for

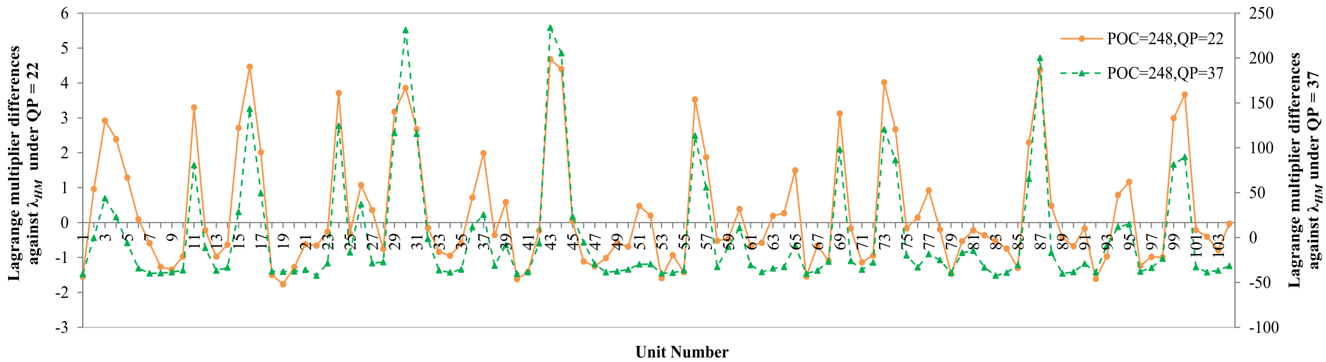

Fig. 5. Lagrange multiplier differences against λ_{HM} for the key frame with POC = 248 in "BasketballDrill".

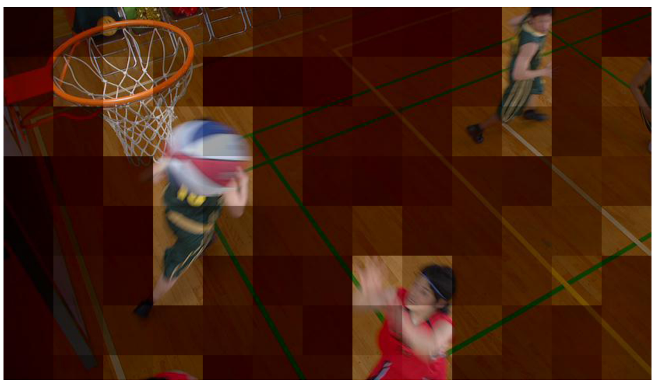

Fig. 6. A visualized representation of CTU-based Lagrange multiplier values in a key frame (POC = 248) of "BasketballDrill" (the darker the smaller and the brighter the larger of the corresponding Lagrange multiplier value in a CTU).

QP values of 22 and 37, respectively. The results are obtained under the LDP configuration and the results under the LDB configuration are very similar thus not detailed here. It can be seen that for the CTUs, the Lagrange multipliers are adapted differently by our proposed method, leading to varying Lagrange multipliers even in one frame (against the same Lagrange multiplier for one frame in the conventional coding, such as λ_{HM}).

For an intuitive illustration, Fig. 6 shows the varying Lagrange multipliers over different CTU locations in a key frame of "BasketballDrill". A brighter CTU corresponds to a larger Lagrange multiplier while a darker region is associated with a smaller one. It can be seen that a smaller Lagrange multiplier is applied to stationary background or still objects and a larger one for a non-stationary region. A smaller Lagrange multiplier tends to select a coding option resulting in a smaller distortion with a higher bit expense, which in turn provides a better reference of higher quality to benefit coding of the subsequent frames. Overall speaking, a little more investment of bit budget in the regions (in a key frame) that will be heavily referenced by the subsequent frames may bring a bigger return of bit saving in coding the corresponding stationary regions in the following key or non-key frames.

C. Coding Complexity

The complexity comparison between HM 13.0 and the proposed method using the adapted Lagrange multiplier is shown in TABLE V in terms of the encoding time under the LDB configuration (similar results under the LDP configuration). Encoding time ratio is obtained as the ratio of geometric means of encoding time. It can be seen that, the encoding time of the proposed method increases only by 1% in average, which is negligible. Although an additional forward motion search is performed in the proposed method, only a very small percentage of time is taken as observed in the experiments. A fast integer-pixel diamond motion search [28] is employed for non-overlapped fixed-size units which simplifies the identification of affected units as demonstrated in Section II.A (other fast motion search methods, such as those in [29] and [30], can also be applied to achieve the same objective). Moreover, the adapted Lagrange multipliers in our method may lead to better prediction results, and then the following residual coding process turns out to be accelerated

TABLE V
ENCODING TIME RATIO OF OUR PROPOSED METHOD UNDER LDB CONFIGURATION

Class	Sequence	Encoding time (in Hours)	
		HM	*Proposed*
B	BasketballDrive	72.84	71.14
	BQTerrace	66.85	59.77
	Cactus	59.49	65.49
	Kimono	38.28	38.47
	ParkScene	34.83	35.40
Encoding time ratio		**99.03%**	
C	BasketballDrill	13.33	13.44
	BQMall	17.40	17.61
	PartyScene	17.00	17.23
	RaceHorses	11.24	11.47
Encoding time ratio		**101.32%**	
D	BasketballPass	4.16	3.63
	BlowingBubbles	3.78	3.85
	BQSquare	4.48	4.57
	RaceHorses	2.39	2.99
Encoding time ratio		**105.17%**	
E	FourPeople	28.23	28.45
	Johnny	24.56	24.94
	KristenAndSara	29.49	29.83
Encoding time ratio		**101.05%**	
F	BaskeballDrillText	13.86	13.94
	ChinaSpeed	28.60	28.71
	SlideEditing	12.42	12.52
	SlideShow	24.09	24.24
Encoding time ratio		**100.64%**	

due to smaller residual errors. For example, if one unit is coded with a smaller Lagrange multiplier producing high reconstruction quality, the following ones referring to this unit will generate smaller residuals, which, in turn, facilitates the following transform, quantization, and entropy coding process to be done faster. Consequently, the overall time may be saved as evidenced by the coding results of some test sequences such as "BasketballPass" shown in TABLE V.

V. Conclusions

In this paper, we have addressed the temporally dependent RDO (TD-RDO) problem under the LD-HCS by considering the hierarchical temporal dependency. Based on the hierarchical temporal propagation relationship under the LD-HCS, the TD-RDO problem is formulated as minimizing the aggregated RD cost of the current coding unit and its temporally related/affected units with the rate dependency decoupled. Then a hierarchical source distortion temporal propagation model is developed to measure the effect of coding one unit, in a key frame and a non-key frame, respectively, on other units. Finally, a hierarchical TD-RDO scheme is proposed and implemented in the way of adapting the Lagrange multiplier. Compared with the HEVC reference software HM 13.0, the proposed approach demonstrates 2.5% and 2.3% BD-rate savings in average under the LDP and LDB configurations, respectively, with a negligible increase in encoding time. For sequences with high temporal dependency such as those under surveillance setting, better performance, i.e., 5.3% and 5.8% BD-rate savings in average are obtained under the LDP and LDB configuration, respectively. Coupled with the MQP scheme, our proposed method can further boost the coding efficiency with the averaged BD-rate savings of 5.4% and 5.0% over the HEVC codec for the LDP and LDB configurations, respectively.

Appendix A

The expected distortions of U_{i+3} and U_{i+4} can be obtained similarly as U_{i+2} in (6), as follows

$$\begin{aligned} E(D_{i+3}) &= P_{i+2,i+3} \cdot D_{i+3}(o_i, o^*_{i+1}, o^*_{i+2}, o^1_{i+3}) \\ &\quad + P_{i,i+3} \cdot D_{i+3}(o_i, o^2_{i+3}) + K_{i+3} \qquad \text{(A1)} \\ E(D_{i+4}) &= P_{i+3,i+4} \cdot D_{i+4}(o_i, o^*_{i+1}, o^*_{i+2}, o^*_{i+3}, o^1_{i+4}) \\ &\quad + P_{i,i+4} \cdot D_{i+4}(o_i, o^2_{i+4}) + K_{i+4} \qquad \text{(A2)} \end{aligned}$$

where $D_{i+3}(o_i, o^*_{i+1}, o^*_{i+2}, o^1_{i+3})$ and $D_{i+4}(o_i, o^*_{i+1}, o^*_{i+2}, o^*_{i+3}, o^1_{i+4})$ are the estimated distortions of U_{i+3} and U_{i+4} when using their immediately previous frame f_{i+2}, f_{i+3} as reference, respectively. $D_{i+3}(o_i, o^2_{i+3})$ and $D_{i+4}(o_i, o^2_{i+4})$ represent the distortions when using their nearest key frame f_i as reference. $K_{i+3} = P_{i-4,i+3} \cdot D_{i+3}(o_{i-4}, o^3_{i+3}) + P_{i-8,i+3} \cdot D_{i+3}(o_{i-8}, o^4_{i+3})$ and $K_{i+4} = P_{i-4,i+4} \cdot D_{i+4}(o_{i-4}, o^3_{i+4}) + P_{i-8,i+4} \cdot D_{i+4}(o_{i-8}, o^4_{i+4})$ are not related to o_i.

To obtain $E(D_{i+3})$ in (A1), two terms related to o_i need to be estimated. First, $D_{i+3}(o_i, o^*_{i+1}, o^*_{i+2}, o^1_{i+3})$ is the distortion of the affected unit in f_{i+3} when using U_{i+2} as reference,

$$\begin{aligned} E(D_{i+3}) &= \begin{pmatrix} P_{i,i+3}\beta_{i,i+3} + P_{i,i+2}\beta_{i,i+2} \cdot P_{i+2,i+3}\beta_{i+2,i+3} \\ +P_{i,i+1}\beta_{i,i+1} \cdot P_{i+1,i+2}\beta_{i+1,i+2} \cdot P_{i+2,i+3}\beta_{i+2,i+3} \end{pmatrix} \cdot D_i(o_i) + C_{i+3} \\ &= \left(\sum_{t=0}^{2} P_{i,i+3-t}\beta_{i,i+3-t} \cdot \prod_{j=i+3-t}^{i+2} P_{j,j+1}\beta_{j,j+1}\right) \cdot D_i(o_i) + C_{i+3} \qquad \text{(A5)} \end{aligned}$$

$$\begin{aligned} D_{i+4}(o_i, o^*_{i+1}, o^*_{i+2}, o^*_{i+3}, o^1_{i+4}) &= \beta_{i+3,i+4} \cdot (E(D_{i+3}) + D^{OMCP}_{i+3\to i+4}) \\ &= \beta_{i+3,i+4} \cdot \left(\sum_{t=0}^{2} P_{i,i+3-t}\beta_{i,i+3-t} \cdot \prod_{j=i+3-t}^{i+2} P_{j,j+1}\beta_{j,j+1}\right) \cdot D_i(o_i) + C'_{i+4} \qquad \text{(A6)} \end{aligned}$$

$$E(D_{i+4}) = \left(\sum_{t=0}^{3} P_{i,i+4-t}\beta_{i,i+4-t} \cdot \prod_{j=i+4-t}^{i+3} P_{j,j+1}\beta_{j,j+1}\right) \cdot D_i(o_i) + C_{i+4} \qquad \text{(A8)}$$

$$\begin{aligned} E(D_{i+8}) &= \left(\sum_{t=0}^{3} P_{i+4,i+8-t}\beta_{i+4,i+8-t} \cdot \prod_{j=i+8-t}^{i+7} P_{j,j+1}\beta_{j,j+1}\right) \cdot E(D_{i+4}) + \tilde{C}_{i+8} \\ &= \prod_{s=0}^{1}\left(\sum_{t=0}^{3} P_{i+4s,i+4s+4-t}\beta_{i+4s,i+4s+4-t} \cdot \prod_{j=i+4s+4-t}^{i+4s+3} P_{j,j+1}\beta_{j,j+1}\right) \cdot D_i(o_i) + C_{i+8} \qquad \text{(A9)} \end{aligned}$$

$$E(D_{i+4m}) = \prod_{s=0}^{m-1}\left(\sum_{t=0}^{3} P_{i+4s,i+4s+4-t}\beta_{i+4s,i+4s+4-t} \cdot \prod_{j=i+4s+4-t}^{i+4s+3} P_{j,j+1}\beta_{j,j+1}\right) \cdot D_i(o_i) + C_{i+4m} \qquad \text{(A10)}$$

which, combined with (14), can be represented as

$$\begin{aligned} &D_{i+3}(o_i, o^*_{i+1}, o^*_{i+2}, o^1_{i+3}) \\ &= \beta_{i+2,i+3} \cdot (E(D_{i+2}) + D^{OMCP}_{i+2\to i+3}) \\ &= \beta_{i+2,i+3} \cdot P_{i+1,i+2}\beta_{i+1,i+2} \cdot P_{i,i+1}\beta_{i,i+1} \cdot D_i(o_i) \\ &\quad + \beta_{i+2,i+3} \cdot P_{i,i+2}\beta_{i,i+2} \cdot D_i(o_i) + C'_{i+3} \end{aligned} \tag{A3}$$

$\beta_{i+2,i+3} = \alpha \cdot e^{-b\cdot R_{i+3}(o^1_{i+3})}$ and $C'_{i+3} = \beta_{i+2,i+3} \cdot (D^{OMCP}_{i+2\to i+3} + C_{i+2})$ are the terms unrelated to o_i. Note that all the affected units can be identified according to the construction of hierarchical temporal propagation chain in Section II. A.

Likewise, the distortion $D_{i+3}(o_i, o^2_{i+3})$ of the affected unit in f_{i+3} when using U_i as reference can be expressed as

$$\begin{aligned} D_{i+3}(o_i, o^2_{i+3}) &= \beta_{i,i+3} \cdot (D_i(o_i) + D^{OMCP}_{i\to i+3}) \\ &= \beta_{i,i+3} \cdot D_i(o_i) + C''_{i+3} \end{aligned} \tag{A4}$$

$\beta_{i,i+3} = \alpha \cdot e^{-b\cdot R_{i+3}(o^2_{i+3})}$ and $C''_{i+3} = \beta_{i,i+3} \cdot D^{OMCP}_{i\to i+3}$ are unrelated to o_i.

By substituting (A3) and (A4) into (A1), the expected distortion of unit U_{i+3} can be obtained in (A5), as shown at the bottom of the previous page, where $C_{i+3} = P_{i+2,i+3} \cdot C'_{i+3} + P_{i,i+3} \cdot C''_{i+3} + K_{i+3}$ is unrelated to o_i.

$E(D_{i+4})$ of (A2) can be obtained in a similar way. First $D_{i+4}(o_i, o^*_{i+1}, o^*_{i+2}, o^*_{i+3}, o^1_{i+4})$ is the distortion of the affected unit in f_{i+4} when using U_{i+3} as reference, which, combined with (A5), can be represented in (A6), as shown at the bottom of the previous page. $\beta_{i+3,i+4} = \alpha \cdot e^{-b\cdot R_{i+4}(o^1_{i+4})}$ and $C'_{i+4} = \beta_{i+3,i+4} \cdot (C_{i+3} + D^{OMCP}_{i+3\to i+4})$ are the terms unrelated to o_i.

In the same way, the distortion $D_{i+4}(o_i, o^2_{i+4})$ of the affected unit in f_{i+4} when using U_i as reference can be obtained as

$$\begin{aligned} D_{i+4}(o_i, o^2_{i+4}) &= \beta_{i,i+4} \cdot (D_i(o_i) + D^{OMCP}_{i\to i+4}) \\ &= \beta_{i,i+4} \cdot D_i(o_i) + C''_{i+4} \end{aligned} \tag{A7}$$

$\beta_{i,i+4} = \alpha \cdot e^{-b\cdot R_{i+4}(o^2_{i+4})}$ and $C''_{i+4} = \beta_{i,i+4} \cdot D^{OMCP}_{i\to i+4}$ are unrelated to o_i. Thus by substituting (A6) and (A7) into (A2), the expected distortion $E(D_{i+4})$ of U_{i+4} can be obtained in (A8), as shown at the bottom of the previous page, where $C_{i+4} = P_{i+3,i+4} \cdot C'_{i+4} + P_{i,i+4} \cdot C''_{i+4} + K_{i+4}$ is unrelated to o_i. As for the estimation of the expected distortions in the following key frames, it can be sequentially obtained in a similar way. For example, combined with $E(D_{i+4})$ in (A8), $E(D_{i+8})$ can be represented in (A9), as shown at the bottom of the previous page, where $\tilde{C}_{i+8}$ and C_{i+8} are both unrelated to o_i. Finally, $E(D_{i+4m})$ in the *m-th* GOP can be obtained in (A10), as shown at the bottom of the previous page, where C_{i+4m} represents all the terms unrelated to o_i.

References

[1] G. J. Sullivan, J.-R. Ohm, W.-J. Han, and T. Wiegand, "Overview of the High Efficiency Video Coding (HEVC) standard," *IEEE Trans. Circuits Syst. Video Technol.*, vol. 22, no. 12, pp. 1649–1668, Dec. 2012.

[2] T. Wiegand, G. J. Sullivan, G. Bjøntegaard, and A. Luthra, "Overview of the H.264/AVC video coding standard," *IEEE Trans. Circuits Syst. Video Technol.*, vol. 13, no. 7, pp. 560–576, Jul. 2003.

[3] L. Shen, Z. Liu, X. Zhang, W. Zhao, and Z. Zhang, "An effective CU size decision method for HEVC encoders," *IEEE Trans. Multimedia*, vol. 15, no. 2, pp. 465–470, Feb. 2013.

[4] P. Helle *et al.*, "Block merge for quadtree-based partitioning in HEVC," *IEEE Trans. Circuits Syst. Video Technol.*, vol. 22, no. 12, pp. 1720–1731, Dec. 2012.

[5] J. Lainema, F. Bossen, W.-J. Han, J. Min, and K. Ugur, "Intra coding of the HEVC standard," *IEEE Trans. Circuits Syst. Video Technol.*, vol. 22, no. 12, pp. 1792–1801, Dec. 2012.

[6] W. Shen *et al.*, "A combined deblocking filter and SAO hardware architecture for HEVC," *IEEE Trans. Multimedia*, vol. 18, no. 6, pp. 1022–1033, Jun. 2016.

[7] I. K. Kim, *High Efficiency Video Coding (HEVC) Test Model 13 (HM13) Encoder Description*, Geneva, Switzerland, document JCTVC-O1002, Nov. 2013.

[8] H. Li, B. Li, and J. Xu, "Rate-distortion optimized reference picture management for High Efficiency Video Coding," *IEEE Trans. Circuits Syst. Video Technol.*, vol. 22, no. 12, pp. 1844–1857, Dec. 2012.

[9] H. Schwarz, D. Marpe, and T. Wiegand, "Analysis of hierarchical B pictures and MCTF," in *Proc. IEEE Int. Conf. Multimedia Expo*, Toronto, ON, Canada, Jul. 2006, pp. 1929–1932.

[10] D. Liu, D. Zhao, X. Ji, and W. Gao, "Dual frame motion compensation with optimal long-term reference frame selection and bit allocation," *IEEE Trans. Circuits Syst. Video Technol.*, vol. 20, no. 3, pp. 325–339, Mar. 2010.

[11] B. Li, J. Xu, D. Zhang, and H. Li, "QP refinement according to Lagrange multiplier for High Efficiency Video Coding," in *Proc. IEEE Int. Symp. Circuits Syst. (ISCAS)*, May 2013, pp. 447–480.

[12] B. Li, D. Zhang, H. Li and J. Xu, *QP Determination by Lambda Value*, Geneva, Switzerland, document JCTVC-I0426, May 2012.

[13] T. Zhao, Z. Wang, and C. W. Chen, "Adaptive quantization parameter cascading in HEVC hierarchical coding," *IEEE Trans. Image Process.*, vol. 25, no. 7, pp. 2997–3009, Jul. 2016.

[14] G. J. Sullivan and T. Wiegand, "Rate-distortion optimization for video compression," *IEEE Signal Process. Mag.*, vol. 15, no. 6, pp. 74–99, Nov. 1998.

[15] A. Ortega and K. Ramchandran, "Rate-distortion methods for image and video compression," *IEEE Signal Process. Mag.*, vol. 15, no. 6, pp. 23–50, Nov. 1998.

[16] X. Li, N. Oertel, A. Hutter, and A. Kaup, "Laplace distribution based Lagrangian rate distortion optimization for hybrid video coding," *IEEE Trans. Circuits Syst. Video Technol.*, vol. 19, no. 2, pp. 193–205, Feb. 2009.

[17] E.-H. Yang and X. Yu, "Rate distortion optimization for H.264 inter-frame coding: A general framework and algorithms," *IEEE Trans. Image Process.*, vol. 16, no. 7, pp. 1774–1784, Jul. 2007.

[18] B. Schumitsch, H. Schwarz, and T. Wiegand, "Optimization of transform coefficient selection and motion vector estimation considering inter-picture dependencies in hybrid video coding," *Proc. SPIE*, vol. 5658, pp. 327–334, Apr. 2005.

[19] C. An and T. Q. Nguyen, "Iterative rate-distortion optimization of H.264 with constant bit rate constraint," *IEEE Trans. Image Process.*, vol. 17, no. 9, pp. 1605–1615, Sep. 2008.

[20] J. Lou and M.-T. Sun, "Rate-distortion optimized rate-allocation for motion-compensated predictive video codecs using PixelRank," *J. Vis. Commun. Image Represent.*, vol. 22, no. 2, pp. 107–116, Feb. 2011.

[21] T. Yang, C. Zhu, X. Fan, and Q. Peng, "Source distortion temporal propagation model for motion compensated video coding optimization," in *Proc. IEEE Int. Conf. Multimedia Expo (ICME)*, Melbourne, VIC, Australia, Jul. 2012, pp. 85–90.

[22] S. Li, C. Zhu, Y. Gao, Y. Zhou, F. Dufaux, and M.-T. Sun, "Lagrangian multiplier adaptation for rate-distortion optimization with inter-frame dependency," *IEEE Trans. Circuits Syst. Video Technol.*, vol. 26, no. 1, pp. 117–129, Jan. 2016.

[23] S. Li, C. Zhu, Y. Gao, Y. Zhou, F. Dufaux, and M.-T. Sun, "Inter-frame dependent rate-distortion optimization using lagrangian multiplier adaption," in *Proc. IEEE Int. Conf. Multimedia Expo (ICME)*, Torino, Italy, Jun. 2015, pp. 1–6.

[24] Y. Gao, C. Zhu, and S. Li, "Hierarchical temporal dependent rate-distortion optimization for low-delay coding," in *Proc. IEEE Int. Symp. Circuits Syst. (ISCAS)*, Montreal, QC, Canada, May 2016, pp. 570–573.

[25] T. A. Cover and J. A. Thomas, *Elements of Information Theory*, 2nd ed. Hoboken, NJ, USA: Wiley, 2006.

[26] F. Bossen, *Common Test Conditions and Software Reference Configurations*, Geneva, Switzerland, document JCTVC-L1100, Jan. 2013.

[27] *An Excel Add-In for Computing Bjontegaard Metric and Its Evolution*, document VCEG-AE07, Jan. 2007.

[28] S. Zhu and K.-K. Ma, “A new diamond search algorithm for fast block-matching motion estimation,” *IEEE Trans. Image Process.*, vol. 9, no. 2, pp. 287–290, Feb. 2000.

[29] C. Zhu, X. Lin, and L.-P. Chau, “An enhanced hexagonal search algorithm for block motion estimation,” in *Proc. IEEE Int. Symp. Circuits Syst. (ISCAS)*, Bangkok, Thailand, May 2003, pp. II-392–II-395.

[30] C. Zhu, X. Lin, and L. P. Chau, “Block motion estimation method,” U.S. Patent 7 457 361 B2, Nov. 25, 2008.

Yanbo Gao received the M.Eng. degree from the Taiyuan University of Science and Technology, Taiyuan, China, in 2013. She is currently pursuing the Ph.D. degree in signal and information processing with the University of Electronic Science and Technology of China, Chengdu, China. Her research interests include video coding, 3D video processing, and light field image coding.

Ce Zhu (M’03–SM’04–F’17) received the B.S. degree from Sichuan University, Chengdu, China, in 1989, and the M.Eng. and Ph.D. degrees from Southeast University, Nanjing, China, in 1992 and 1994, respectively, all in electronic and information engineering. He did post-doctoral research with The Chinese University of Hong Kong in 1995, the City University of Hong Kong, and The University of Melbourne, Australia from 1996 to 1998. He was with Nanyang Technological University, Singapore, from 1998 to 2012, where he was a Research Fellow, a Program Manager, an Assistant Professor, and then promoted to an Associate Professor in 2005. He has also held visiting positions with Queen Mary, University of London, and Nagoya University. He is currently a Professor with the University of Electronic Science and Technology of China, Chengdu, China.

As a Lead Editor, he has edited three books and contributed four book chapters. He holds over 30 patents issued or pending, and has contributed over 40 proposals (over 20 adopted) to the international standardization bodies of JCT-3V (3D-HEVC) and MPEG Internet video coding and the China AVS standardization (mainly on encoding optimization with proposed techniques adopted in the standard test model and reference software). His research interests include video coding and communications, video analysis and processing, 3D video, visual perception, and applications. He has authored or co-authored over 150 publications.

Dr. Zhu is an Elected Member of the Multimedia Signal Processing Technical Committee (MMSP-TC) of the IEEE Signal Processing Society, the Chair of the Webmaster Subcommittee of MMSP-TC, and an Elected Member of the Multimedia Systems and Applications Technical Committee of the IEEE Circuits and Systems Society. He is an IEEE Broadcast Technology Society’s Distinguished Lecturer. He is a Co-Chair of the Interest Group of Multimedia Processing for Communications of Technical Committee on Multimedia Communications, IEEE Communications Society and the Chair of the Special Interest Group on Big Multimedia of Technical Committee on Multimedia Computing, the IEEE Computer Society. He has served on technical/program committees, organizing committees, and as the Track/Area/Session Chair for around 60 international conferences, including as a Technical Program Co-Chair of the IEEE ICME 2017. He has also given tutorials at international conferences, such as the IEEE ISCAS 2015, VCIP 2014, and PCM 2014, and has delivered keynote speeches at a few international conferences. He has served on the editorial boards of a few journals, including as an Associate Editor of the IEEE TRANSACTIONS ON CIRCUITS AND SYSTEMS FOR VIDEO TECHNOLOGY, the IEEE TRANSACTIONS ON IMAGE PROCESSING, the IEEE TRANSACTIONS ON BROADCASTING, and the IEEE SIGNAL PROCESSING LETTERS, an Editor of the IEEE COMMUNICATIONS SURVEYS AND TUTORIALS, and an Area Editor of *Signal Processing: Image Communication*. He has also served as a Guest Editor for a few special issues in international journals.

He is a Fellow of the IEEE and the IET. He was a co-recipient of two best paper awards (as the first author), the one student paper award, and a Finalist of the World’s FIRST 10K Best Paper Award (top 3%), at the IEEE BMSB 2014, IIH-MSP 2013, MobiMedia 2011, and ICME 2017, respectively.

Shuai Li received the B.Eng. degree from Yantai University, Yantai, China, in 2011, and the M.Eng. degree from Tianjin University, Tianjin, China, in 2014. He is currently pursuing the Ph.D. degree in computer science with the University of Wollongong, Australia. He was with the University of Electronic Science and Technology of China as a Research Assistant from 2014 to 2015.

His research interests include image/video coding, 3D video processing, and computer vision. He was a co-recipient of two best paper awards at the IEEE BMSB 2014 and IIH-MSP 2013, respectively.

Tianwu Yang received the Ph.D. degree in traffic information engineering and control from Southwest Jiaotong University, Chengdu, China, in 2007. He is currently a Research Scientist with the Advanced Robotics and Intelligent Control Centre, Singapore Polytechnic, Singapore. He serves as a Technical Consultant of RoboCup Junior CoSpace League. His research interests include video coding, image processing, artificial intelligence, educational robotics, and human–robot interaction.